Drug Design, Development and Therapy

Dovepress
Taylor & Francis Group

Open Access Full Text Article

ORIGINAL RESEARCH

Comparative Protective Effects of ATP and TPP Against Olaparib-Induced Ovarian Injury in Rats: Insights from Biochemical Parameters, Histopathology, and IRE1α, Cleaved Caspase-3, LC3B, and NF-κB p65 Double Immunofluorescence

Seyma Ilayda Paltaci[1], Nesrin Yilmaz[1], Sukran Kozali Uzun[1], Bulent Yavuzer[2], Taha Abdulkadir Coban[3], Mustafa Ozkaraca[4], Ali Gungor[5], Kamandar Yaqubov[6], Halis Suleyman[2,7]

[1]Department of Obstetrics and Gynecology, Faculty of Medicine, Erzincan Binali Yıldırım University, Erzincan, Turkey; [2]Department of Pharmacology, Faculty of Medicine, Erzincan Binali Yıldırım University, Erzincan, Turkey; [3]Department of Medical Biochemistry, Faculty of Medicine, Erzincan Binali Yıldırım University, Erzincan, Turkey; [4]Department of Pathology, Faculty of Veterinary Medicine, Sivas Cumhuriyet University, Sivas, Turkey; [5]Laboratory and Veterinary Health Program, Vocational School of Health Services, Osmaniye Korkut Ata University, Osmaniye, Turkey; [6]Department of Pharmacology, Azerbaijan Medical University, Baku, Azerbaijan; [7]Department of Pharmacology, Faculty of Medicine, Ataturk University, Erzurum, Turkey

Correspondence: Halis Suleyman, Department of Pharmacology, Faculty of Medicine, Erzincan Binali Yıldırım University, Erzincan, Turkey, Tel +90 530 9211909, Fax +90 446 2261819, Email hsuleyman@erzincan.edu.tr

Drug Design, Development and Therapy downloaded from https://www.dovepress.com/
For personal use only.

Background: Olaparib is a poly(ADP-ribose) polymerase (PARP) inhibitor used to treat several malignancies. Previous studies have reported that olaparib may induce ovarian injury by elevating reactive oxygen species and impairing cellular energy homeostasis. ATP is a central regulator of intracellular energy balance and antioxidant defense, whereas thiamine pyrophosphate (TPP), the active form of vitamin B1, supports ATP biosynthesis and possesses antioxidant and anti-inflammatory properties. This study compared the protective effects of ATP and TPP against olaparib-induced ovarian injury in rats.

Methods: Twenty-four female Wistar albino rats were randomly assigned to four groups (n=6 each): healthy control (HG), olaparib-only (OLP), ATP plus olaparib (ATOL), and TPP plus olaparib (TPOL). Olaparib (100 mg/kg, orally, twice daily), ATP (5 mg/kg, intraperitoneally, once daily), and TPP (25 mg/kg, intraperitoneally, once daily) were administered for 14 consecutive days. Ovarian tissue levels of oxidant (MDA), antioxidants (tGSH, SOD, CAT), and pro-inflammatory cytokine (IL-6) were determined. Tissue specimens underwent histopathological (follicular and parenchymal degeneration) and double immunofluorescence analyses (IRE1α, cleaved Caspase-3, LC3B, and NF-κB p65 immunopositivity).

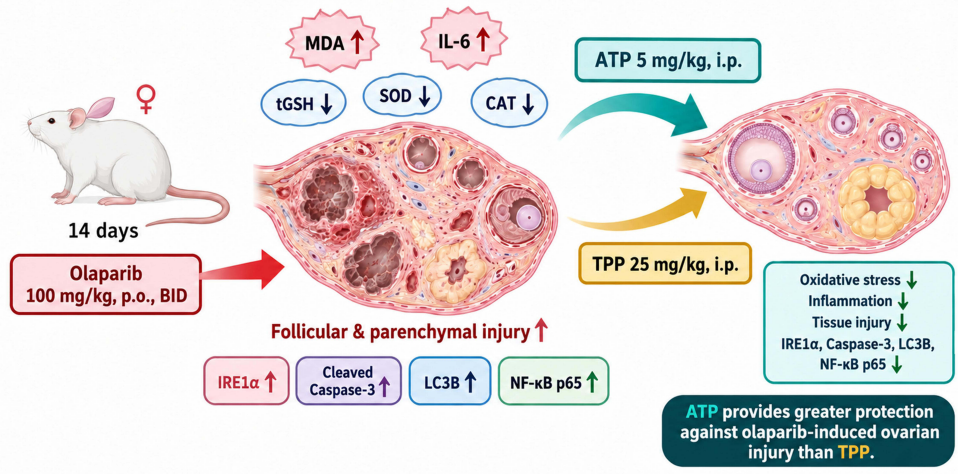
Results: Olaparib significantly increased oxidant and pro-inflammatory cytokine levels and decreased antioxidant levels. Histopathology revealed severe follicular and parenchymal degeneration, and immunofluorescence analysis showed significantly increased IRE1α, cleaved Caspase-3, LC3B, and NF-κB p65 immunopositivity. Both ATP and TPP pre-treatment significantly attenuated olaparib-induced oxidative stress, inflammatory responses, histopathological injury, and cellular stress marker immunopositivity. ATP demonstrated a more pronounced protective effect than TPP, particularly regarding follicular degeneration suppression and LC3B and NF-κB p65 immunopositivity.

Conclusion: Olaparib induced ovarian injury accompanied by oxidative stress, cytokine-mediated inflammation, IRE1α-related endoplasmic reticulum stress, cleaved Caspase-3-related apoptosis, LC3B-related autophagy, and NF-κB-related inflammatory signaling. Both ATP and TPP attenuated olaparib-associated injury, with greater effects for ATP. These findings suggest that maintenance of cellular energy homeostasis may represent a promising strategy for attenuating PARP inhibitor-induced ovarian injury.

https://doi.org/10.2147/DDDT.S634516
Received: 21 June 2026
Accepted: 16 September 2026
Published: 26 September 2026

© 2026 Paltaci et al. This work is published and licensed by Dove Medical Press Limited. The full terms of this license are available at https://www.dovepress.com/terms.php and incorporate the Creative Commons Attribution – Non Commercial (unported, v4.0) License (http://creativecommons.org/licenses/by-nc/4.0/). By accessing the work you hereby accept the Terms. Non-commercial uses of the work are permitted without any further permission from Dove Medical Press Limited, provided the work is properly attributed. For permission for commercial use of this work, please see paragraphs 4.2 and 5 of our Terms (https://www.dovepress.com/terms.php).

Graphical Abstract



Keywords: adenosine triphosphate, apoptosis, autophagy, endoplasmic reticulum stress, inflammation, olaparib, ovarian diseases/chemically induced, oxidative stress, rats, thiamine pyrophosphate

Introduction

Poly (ADP-ribose) polymerases (PARPs) constitute a family of enzymes that play a crucial role in maintaining genomic stability by initiating repair in response to DNA single-strand breaks.[1] PARP inhibitors exert their effects by inhibiting these enzymes, thereby inducing double-strand breaks, promoting the accumulation of DNA damage, and ultimately leading to cell death.[2] Olaparib is an anticancer agent that exerts its therapeutic effects through the inhibition of PARP1, PARP2, and PARP3 in cells.[3] Olaparib is widely used in the treatment of ovarian, primary peritoneal, metastatic pancreatic, metastatic castration-resistant prostate, and HER-2-negative breast cancers.[4] However, treatment-related adverse effects, including fatigue, nausea, vomiting, anemia, diarrhea, dyspepsia, and hematological toxicity, have been reported.[5,6] In addition to exacerbating DNA damage, PARP inhibitors may also modulate angiogenic pathways; inhibition of PARP has been shown to suppress VEGF-mediated angiogenesis and endothelial function in various experimental models.[7–9] In mice, olaparib has been shown to directly reduce ovarian reserve and follicular survival, accompanied by granulosa cell dysfunction, in addition to impairing downstream reproductive outcomes such as oocyte retrieval and fertilization rates.[10] In rats, olaparib has similarly been shown to reduce primordial follicle numbers, but this effect was significant only in genetically susceptible Brca1-mutant animals and did not reach significance in wild-type rats at the same dose.[11] Thus, the available evidence remains insufficient to establish that olaparib directly injures ovarian tissue in genetically normal rats, highlighting the need for further characterization of its effects on ovarian tissue. Moreover, PARP1 inhibition has been shown to elevate reactive oxygen species (ROS) levels in ovarian cancer cells,[12] with olaparib specifically reported to induce a rapid increase in mitochondrial ROS.[13]

Studies have also shown that olaparib elevates interleukin-6 (IL-6) levels in breast cancer cells and enhances nuclear factor-kappa B (NF-κB) expression in ovarian cancer.[14,15] NF-κB, which can be activated by oxidative stress, is responsible for the transcription of genes encoding proinflammatory cytokines, chemokines, and acute-phase proteins.[16,17] IL-6, in turn, is a proinflammatory cytokine that plays a key role in tissue homeostasis.[18]

The increase in ROS associated with olaparib administration may trigger endoplasmic reticulum (ER) stress, leading to activation of the unfolded protein response (UPR) and inositol-requiring enzyme 1 alpha (IRE1α).[19–21] Although the

UPR primarily aims to promote adaptation to ER stress and support cell survival, under severe or prolonged stress conditions it can initiate apoptosis, thereby eliminating the damaged cell.[21]

Olaparib has been reported to impair mitochondrial function in ovarian cancer cells, thereby inducing mitochondrial fission and subsequently increasing caspase-3 activation.[19] Caspases are cysteine proteases involved in cell death, inflammation, and cellular differentiation, and caspase-3 serves as a key executioner caspase responsible for the proteolytic cleavage of cellular substrates and the subsequent formation of apoptotic bodies.[22–24] Increased caspase-3 activity and PARP cleavage have been observed in olaparib-treated cell models, indicating that olaparib can promote apoptosis via caspase-3 in certain tumor cells.[25,26]

Beyond apoptosis, olaparib and other PARP inhibitors have been shown to induce autophagy in breast cancer cells harboring BRCA1 mutations and BRCA1 allelic loss.[4] Autophagy is a cellular process that is upregulated in response to various stress stimuli, including hypoxia, ROS, DNA damage, and pathogens.[27] Excessive activation of autophagy may result in cell death.[1] Notably, olaparib upregulates microtubule-associated protein 1 light chain 3 beta (LC3B) expression, a key molecular marker of autophagy.[28]

Olaparib has been reported to not only increase mitochondrial oxidative stress but also reduce intracellular ATP levels.[19] Excessive ROS production is known to impair ATP synthesis and may induce mitochondrial damage.[29] These findings suggest that ATP depletion may represent one of the primary mechanisms underlying the pathogenesis of olaparib-associated oxidative stress. Indeed, several studies have demonstrated an association between oxidative stress and ATP depletion.[30,31]

Adenosine triphosphate (ATP), investigated in this study for its potential protective effects against olaparib-induced ovarian injury, is a nucleoside triphosphate composed of a nitrogenous base, a ribose sugar, and three phosphate groups.[32] ATP provides the energy required for the synthesis of antioxidants.[29] There is growing evidence indicating that ATP suppresses both oxidative stress and inflammatory responses.[33] Conversely, a reduction in ATP levels is known to activate AMP-activated protein kinase (AMPK), thereby promoting the induction of autophagy.[34]

Thiamine pyrophosphate (TPP), the other molecule investigated in this study for its potential protective effects against olaparib-induced ovarian injury, is the phosphorylated and biologically active form of vitamin B1 (thiamine) found in tissues.[35,36] TPP is known to serve as a coenzyme for more than twenty enzymes.[35] It plays a role in reactions involved in ATP production and the reduction of oxidative stress.[37] Experimental studies have demonstrated that TPP suppresses excessive production of proinflammatory cytokines and exhibits antioxidant properties.[38] Thiamine deficiency has been shown to induce autophagosome accumulation and increase LC3B expression in neurons, whereas thiamine administration has been demonstrated to reduce LC3B levels.[39] Moreover, a preclinical study demonstrated that ER stress induced by a high-carbohydrate diet was alleviated by thiamine administration.[40]

Collectively, these findings suggest that ATP and TPP may be beneficial in the management of olaparib-induced ovarian damage. A recent study reported the comparative protective effects of ATP and melatonin against olaparib-induced hepatic injury in male rats,[41] and the present study extends this line of investigation to olaparib-induced ovarian injury in female rats, comparing ATP with TPP as an alternative protective agent. To the best of our knowledge, no study has directly and comparatively evaluated the protective effects of ATP and TPP against oxidative and cellular stress responses induced by olaparib in ovarian tissue. Therefore, the present study aimed to investigate and comparatively evaluate the protective effects of ATP and TPP against olaparib-induced ovarian injury in rats through biochemical, histopathological, and double immunofluorescence analyses.

Materials and Methods

Animals and Housing

To minimize biological variability among groups, only female Wistar albino rats aged 9–10 weeks and weighing 265–277 g were included in the study, resulting in a total sample size of 24 animals. The entire animal cohort was sourced exclusively from the Experimental Animal Application and Research Center of Erzincan Binali Yıldırım University (EBYU), located in Erzincan, Turkey. Using a stratified randomization procedure designed to equalize mean body weights across groups at baseline, the animals were distributed into four groups of six rats each. A seven-day habituation

phase was allowed for all animals prior to the onset of any experimental intervention. Throughout acclimatization and the subsequent experimental period, the rats were maintained in standard wire-mesh laboratory cages with internal dimensions of 35 cm × 55 cm (floor area: 1925 cm^2) and a height of 20 cm, accommodating six animals per cage.

Husbandry conditions remained constant throughout the study. The animals were kept on a 12-hour light/dark cycle at 22°C ± 2°C and 30–70% relative humidity, with free access to standard rodent pellets (Bayramoglu Feed and Flour Industry Inc., Erzurum, Turkey) and tap water. Following the seven-day habituation period and immediately prior to randomization, each animal underwent a general health assessment based on direct observation by a trained researcher. The assessment included general appearance, posture, spontaneous locomotor activity, responsiveness to handling, grooming and coat condition, food and water intake, and the presence of visible injuries or other overt signs of illness. No abnormalities were observed in any of the 24 animals, and all animals were considered to be in good health prior to randomization.

All experimental procedures were performed in the accredited laboratory of the Experimental Animal Application and Research Center of EBYU. All experimental procedures were conducted in accordance with European Parliament Directive 2010/63/EU governing the protection of animals used for scientific purposes,[42] and reporting adhered to the ARRIVE 2.0 guidelines.[43] Consistent with the refinement principle of ethical animal research, all feasible measures were implemented to reduce pain, suffering, and distress experienced by the study animals. Animals were monitored daily throughout the study for general health status and signs of discomfort. Furthermore, the number of animals used was kept to the minimum necessary to achieve the scientific objectives of the study while complying with ethical principles for animal experimentation.

Chemicals and Reagents

All chemicals and reagents used in this study were obtained from commercial suppliers. Thiopental sodium (Pental Sodyum®, 0.5 g powder for solution for injection; Cat. No. 8699508270385) was supplied by Menarini Health and Pharmaceutical Industry Trade Inc. (Istanbul, Turkey). Olaparib (Lynparza®, 150 mg film-coated tablets; Cat. No. 8699786092921) was supplied by AstraZeneca Pharmaceuticals Industry and Trade Ltd. Co. (Istanbul, Turkey). Adenosine triphosphate sodium (Sodium Adenosine Triphosphate–Darnytsia®, 10 mg/mL solution for injection; Cat. No. 4823006406180) was obtained from Darnytsia Pharmaceutical Co. (Kyiv, Ukraine). Thiamine pyrophosphate (Cocarboxylase hydrochloride®, 50 mg/2 mL solution for injection; Cat. No. 4820011070436) was obtained from BioPharma (Kyiv, Ukraine).

Experimental Design and Randomization

The determination of sample size was guided by rigorous application of the 4R framework (Reduction, Refinement, Replacement, and Responsibility), a set of principles collectively aimed at limiting animal use to the lowest number compatible with scientific validity and reproducibility.[44] Exclusion criteria were defined a priori for the pre-experimental period, the experimental period, and the post-experimental period. At the pre-experimental stage, animals displaying abnormal body posture, diminished spontaneous locomotor activity, or visible injuries attributable to aggressive conspecific interactions within the home cage were flagged for potential exclusion. Any individual satisfying one or more of the aforementioned criteria was designated for exclusion prior to the randomization process and before the administration of any study compound.

The exclusion criteria applicable during and after the experimental period included the following: mortality occurring before predefined experimental endpoints were reached; clinically significant adverse events attributable to anesthetic procedures or the administration of study agents; procedural failures including unsuccessful intragastric gavage delivery or extravasation at the injection site; deviation from the predefined treatment protocol or failure to complete the full course of compound administration; a reduction in body weight exceeding 15% of the individually recorded baseline value; observable clinical signs consistent with dehydration or the presence of systemic illness; and intractable pain or severe psychological distress evidenced by continuous vocalization or self-directed injurious behavior. Furthermore, structural compromise of tissue specimens occurring during collection or laboratory processing, of a nature sufficient to

undermine the reliability or analytical accuracy of biochemical, histopathological, or double immunofluorescence assessments, was likewise regarded as a legitimate basis for exclusion.

Animals were monitored for the predefined exclusion criteria throughout the experimental period and during tissue collection and sample processing. No animals met the exclusion criteria; therefore, all 24 animals were included in the final analysis. A formal a priori power analysis was not performed. Group sizes were determined based on comparable previously published experimental studies and the Reduction principle of animal research. An independent researcher assigned the animals to groups using a computer-generated random sequence. Each cage and animal was assigned a unique numerical identifier that remained unchanged throughout the experiment. Investigators performing the biochemical, histopathological, and double immunofluorescence analyses were blinded to group allocation.

Experimental Groups

Animals were randomly assigned to four experimental groups (n = 6 per group): healthy control (HG); olaparib-only (OLP; 100 mg/kg, oral); ATP pretreatment combined with olaparib (ATOL; ATP 5 mg/kg, intraperitoneally and olaparib 100 mg/kg, oral); and TPP pretreatment combined with olaparib (TPOL; TPP 25 mg/kg, intraperitoneally and olaparib 100 mg/kg, oral).

Experimental Procedure

ATP was administered intraperitoneally (i.p.) to the ATOL group (n = 6) at a dose of 5 mg/kg once daily.[45] TPP was administered i.p. to the TPOL group (n = 6) at a dose of 25 mg/kg once daily.[46] The HG and OLP groups (n = 6 each) received an equivalent volume of distilled water via the same route. One hour after these administrations, olaparib was administered orally by gavage to the OLP, ATOL, and TPOL groups at a dose of 100 mg/kg twice daily. Treatments were continued for 14 consecutive days. The olaparib dosing regimen (100 mg/kg orally twice daily; total daily dose, 200 mg/kg/day) was consistent with previously published Wistar rat models of olaparib-associated gastric and hepatic injury employing the same dose, route, administration frequency, and treatment duration.[41,47] High-dose olaparib regimens have also been shown to produce measurable systemic exposure and biological activity in other preclinical settings. In a mouse tumor-prevention model, administration of olaparib at 200 mg/kg diet resulted in a measured plasma concentration of approximately 36 nM and delayed tumor development.[48] In mouse xenograft models, Sun et al reported a plasma AUC0–24h of 11.28 μg h/mL following olaparib administration at 100 mg/kg once daily and an AUC0–12h of 15.59 μg h/mL following 67 mg/kg twice-daily administration.[49] For clinical context, a population pharmacokinetic analysis in patients with cancer demonstrated a steady-state geometric mean AUC of 49.0 μg h/mL and Cmax of 7.7 μg/mL following the therapeutic olaparib tablet regimen of 300 mg twice daily.[50] Based on the aforementioned preclinical evidence, the high-dose regimen used in the present study was selected to establish an ovarian injury model within a defined treatment period, thereby enabling evaluation of the protective effects of ATP and TPP.

At the end of the treatment period, deep surgical anesthesia was induced in all animals by a single intraperitoneal injection of thiopental sodium (50 mg/kg). Loss of the corneal and pedal withdrawal reflexes was used to confirm adequate anesthetic depth before proceeding with any further intervention. Following confirmation of areflexia, euthanasia was carried out by cervical dislocation under continued deep anesthesia, and the absence of respiration and heartbeat was taken as confirmation of death. Ovarian tissues were then surgically excised and harvested. This anesthesia and euthanasia protocol conformed to Annex IV of European Parliament Directive 2010/63/EU[42] and to the 2020 AVMA Guidelines for the Euthanasia of Animals,[51] thereby minimizing the potential for pain and distress during the terminal procedure. Tissue levels of malondialdehyde (MDA), total glutathione (tGSH), superoxide dismutase (SOD), catalase (CAT), and interleukin-6 (IL-6) were subsequently determined from the harvested tissues. Ovarian tissues were additionally processed for histopathological (follicular and parenchymal degeneration) and double immunofluorescence (IRE1α, cleaved Caspase-3, LC3B, and NF-κB p65) examination. All experimental findings were evaluated by intergroup comparison.

Biochemical Analyses

Preparation of Ovarian Tissue Homogenates

Ovarian tissues were retrieved from all animals immediately after euthanasia, and 100 mg aliquots were obtained by weighing on a precision analytical balance. Prior to further processing, each aliquot was immersed in ice-cold physiological saline (0.9% NaCl) to clear surface debris and residual erythrocytes. Tissue fragments were snap-frozen in liquid nitrogen and ground using a mortar and pestle maintained at dry-ice temperature. The cryopulverized material was homogenized in phosphate-buffered saline (PBS, pH 7.4) at a 1:10 tissue-to-buffer ratio (w/v) to yield a crude homogenate. Each homogenate was vortexed for 10s and centrifuged at 10,000 × g for 20 min at 4°C. The clarified supernatant fraction was transferred to fresh tubes and stored at −80°C until biochemical analyses were performed. Assay results for MDA and tGSH were normalized to total protein content and reported as nmol/mg protein, whereas SOD and CAT levels were similarly normalized and expressed as ng/mg protein.

Determination of Ovarian Tissue MDA, tGSH, SOD, CAT, and Protein Levels

Tissue levels of MDA and tGSH, together with the levels of SOD and CAT, were determined using rat-specific commercial enzyme-linked immunosorbent assay (ELISA) kits obtained from Shanghai YL Biotech Co., Ltd. (Shanghai, China): MDA (Cat. No. YLA0029RA), tGSH (Cat. No. YLA0121RA), SOD (Cat. No. YLA0115RA), and CAT (Cat. No. YLA0123RA). All measurements were performed according to the manufacturer's instructions. Total protein concentration was determined using the Bradford assay with Coomassie Brilliant Blue G-250 dye (Sigma-Aldrich Chemie GmbH, Taufkirchen, Germany; Cat. No. 115444), and absorbance was measured at 595 nm.[52]

Determination of Ovarian Tissue IL-6 Levels

Tissue levels of interleukin-6 (IL-6; ng/L) were determined using a commercially available ELISA kit (Cat. No. YLA0031RA; Shanghai YL Biotech Co., Ltd., Shanghai, China) in accordance with the manufacturer's instructions.

Histopathological Evaluation

Ovarian tissue specimens were immersion-fixed in 10% neutral buffered formalin to maintain the structural integrity of tissues for light microscopic analysis. After adequate fixation, specimens were transferred into tissue cassettes and rinsed under continuously running tap water for 24 hours to eliminate residual fixative. Tissues were subsequently processed through a graded ethanol series (70%, 90%, and 100%) for dehydration, followed by xylene clearing and paraffin embedding. From the paraffin blocks, serial sections of 4–5 µm were prepared with a rotary microtome, mounted on glass slides, and subjected to hematoxylin and eosin (H&E) staining for histopathological examination.

Tissue specimens from six animals per experimental group (n = 6) were included in the analysis, and one paraffin section from each animal was used for morphological evaluation. For each section, one representative field was randomly selected and examined under 40× objective magnification to minimize sampling bias. Accordingly, six photomicrographs were captured per experimental group, with each image representing one individual animal. Images were acquired using an Axiolab 5 microscope, an Axiocam 305 color camera, and a Colibri 3 LED illumination system (Carl Zeiss Microscopy GmbH, Jena, Germany); image acquisition and processing were carried out using ZEISS ZEN 3.1 (Blue Edition) software (Carl Zeiss Microscopy GmbH, Jena, Germany).

Histopathological injury was assessed based primarily on two morphological criteria: follicular degeneration and parenchymal degeneration within the ovarian tissue. Tissue damage was graded according to a four-point semi-quantitative scale detailed in Table 1, with scores of 0, 1, 2, and 3 corresponding to absent, mild, moderate, and severe injury, respectively. To reduce observer-related bias, histological evaluation was performed by one experienced pathologist who was blinded to group assignments throughout the assessment process.

Double Immunofluorescence Method

Five-micrometer-thick tissue sections mounted on poly-L-lysine-coated slides were deparaffinized through xylene and rehydrated through a graded alcohol series, followed by washing with phosphate-buffered saline (PBS). Antigen retrieval was performed in citrate buffer (pH 6.0) at 800 W for 2×5 min. The sections were washed twice with PBS for 10 min

Table 1 Semi-Quantitative Histopathological Grading of Follicular and Parenchymal Degeneration in Ovarian Tissue Across Experimental Groups

Group	Follicular Degeneration Score	Parenchymal Degeneration Score
HG	0 (0–0)	0 (0–0)
OLP	3 (2–3)[a]	3 (2–3)[a]
ATOL	0 (0–1)[b]	1 (0–2)[a, b]
TPOL	2 (1–2)[a, b, c]	1 (1–2)[a, b]

Notes: Histopathological scores are presented as median (min–max). Both follicular and parenchymal degeneration were assessed using a four-point grading scale: 0 = absent, 1 = mild, 2 = moderate, 3 = severe.[a] indicates $p < 0.05$, vs HG;[b] indicates $p < 0.05$, vs OLP;[c] indicates $p < 0.05$, vs ATOL. Pairwise comparisons were performed using the Mann–Whitney *U*-test (asymptotic, two-tailed) with Bonferroni correction applied for multiple comparisons. Each experimental group comprised six animals (n = 6).
Abbreviations: HG, healthy group; OLP, olaparib-only group; ATOL, ATP + olaparib group; TPOL, TPP + olaparib group; ATP, adenosine triphosphate; TPP, thiamine pyrophosphate.

each time and subsequently immersed in PBS / gelatin (0.25%) / Triton X-100 (0.25%) solution for 10 min to permeabilize the tissue and reduce nonspecific binding. Nonspecific protein binding was suppressed by incubating the sections in 5% bovine serum albumin (BSA) for 1 h.

After blocking, the sections were sequentially incubated with two pairs of primary antibodies on the same slide. Between incubations, the sections were washed twice with PBS for 10 min and blocked with 5% BSA for 1 h to prevent cross-reactivity. The first pair comprised monoclonal anti-IRE1α (Santa Cruz Biotechnology, Inc., Dallas, TX, USA; Cat. No. sc-390960) and polyclonal anti-cleaved Caspase-3 (Asp175) (Thermo Fisher Scientific, Inc., Waltham, MA, USA; Cat. No. PA5-114687) antibodies. The second pair comprised monoclonal anti-LC3B (Santa Cruz Biotechnology, Inc., Dallas, TX, USA; Cat. No. sc-271625) and polyclonal anti-NF-κB p65 (Affinity Biosciences, Cincinnati, OH, USA; Cat. No. AF5006) antibodies. All primary antibodies were applied at a 1/200 dilution, and the sections were incubated overnight at 4°C. After each incubation step, the sections were washed twice with PBS for 10 min each time. Sections processed without primary antibody treatment were included as negative controls.

Following primary antibody incubation, the sections were incubated for 45 min with a secondary antibody cocktail prepared in 1% BSA and diluted 1/100, consisting of equal proportions of Goat Anti-Mouse FITC (Jackson ImmunoResearch Laboratories, Inc., West Grove, PA, USA; Cat. No. 115–095-003) and Anti-Rabbit Alexa Fluor 594 (Cell Signaling Technology, Inc., Danvers, MA, USA; Cat. No. 8889S). The sections were subsequently washed twice with PBS for 10 min each time and treated with 10 mM $CuSO_4$/50 mM NH_4Cl solution for 10 min to reduce autofluorescence. Following a final wash with distilled water, DAPI (4′,6-diamidino-2-phenylindole) was applied for nuclear counterstaining, and the sections were examined at 40× magnification using an Axiolab 5 fluorescence microscope, an Axiocam 305 color camera, and a Colibri 3 light source (all from Carl Zeiss Microscopy GmbH, Jena, Germany).

During image evaluation, IRE1α and LC3B immunopositivities were visualized as green fluorescence, whereas cleaved Caspase-3 and NF-κB p65 immunopositivities were visualized as red fluorescence. Immunoreactivity was scored using a five-point semi-quantitative system: absent (0), mild (1), moderate (2), severe (3), and very severe (4), with ZEISS ZEN 3.1 (Blue Edition) software (Carl Zeiss Microscopy GmbH, Jena, Germany). All scoring was performed by a single experienced observer who was blinded to group allocation.

Statistical Analysis

All statistical procedures were carried out using IBM SPSS Statistics for Windows (Version 27.0; IBM Corp., Armonk, NY, USA; 2020). Biochemical findings are expressed as mean ± standard error of the mean, and all graphical representations were produced with GraphPad Prism (Version 8.0.1; GraphPad Software, Inc., San Diego, CA, USA; 2018). Prior to inferential testing, the normality of the biochemical data distribution was assessed by the Shapiro–Wilk test (Supplementary Table 1), whereas variance homogeneity across groups was evaluated by Levene's test (Supplementary Table 2). In cases where both assumptions were fulfilled, intergroup differences were examined by one-

way analysis of variance, and pairwise comparisons were subsequently conducted using Tukey's Honestly Significant Difference (HSD) test (Supplementary Table 3). When the normality assumption was met but variance homogeneity could not be confirmed, Welch's analysis of variance was employed, with post hoc multiple comparisons carried out using the Games–Howell test (Supplementary Table 3).

Because histopathological damage scores and double immunofluorescence signal intensity ratings constitute ordinal variables, parametric testing was not applicable to these data. Pairwise intergroup comparisons for these variables were conducted using the two-tailed Mann–Whitney *U*-test, with Bonferroni correction applied to account for multiple comparisons. Histopathological and double immunofluorescence data are reported as median (minimum–maximum). A p value below 0.05 was regarded as statistically significant for all tests applied in this study.

Ethical Approval

The study protocol was reviewed and approved by the Local Ethics Committee for Animal Experiments of Erzincan Binali Yıldırım University (Erzincan, Turkey; Approval No., 9; Session No., 01/2026; Approval Date, 29.01.2026).

Results

Biochemical Findings

Ovarian Tissue MDA and tGSH Levels

As shown in Figure 1, ovarian MDA levels were significantly increased in the OLP group (4.59 ± 0.07) compared with the HG group (2.38 ± 0.06) ($p < 0.001$). Both ATP and TPP pre-treatment significantly attenuated the olaparib-induced increase in MDA levels (ATOL, 2.57 ± 0.06; TPOL, 2.66 ± 0.05; both vs OLP, $p < 0.001$). No significant difference was detected between the ATOL and TPOL groups ($p = 0.765$). While MDA levels in the ATOL group did not differ significantly from those of the HG group ($p = 0.136$), TPOL animals exhibited significantly higher MDA levels than healthy controls ($p = 0.019$).

Olaparib administration significantly decreased ovarian tGSH levels from 6.43 ± 0.06 in the HG group to 3.56 ± 0.10 in the OLP group ($p < 0.001$). ATP and TPP pre-treatment significantly attenuated the olaparib-induced decrease in tGSH levels (ATOL, 6.17 ± 0.10; TPOL, 6.14 ± 0.11; both vs OLP, $p < 0.001$). No significant difference was observed between the two treatment groups ($p = 0.997$). Furthermore, tGSH levels in both groups remained statistically comparable to those observed in healthy animals (ATOL vs HG, $p = 0.237$; TPOL vs HG, $p = 0.170$) (Figure 1).

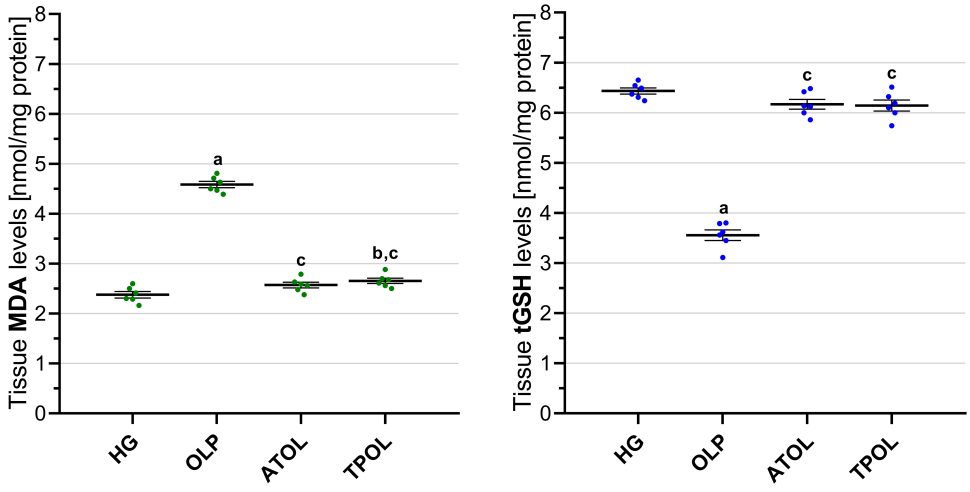


Figure 1 Effects of ATP, TPP, and olaparib on MDA and tGSH levels in rat ovarian tissue.
Notes: Values represent mean ± SEM. Intergroup differences were assessed by one-way ANOVA followed by Tukey's honestly significant difference (HSD) post hoc test. [a] $p < 0.001$ vs HG; [b] $p < 0.05$ vs HG; [c] $p < 0.001$ vs OLP. n = 6 per group.
Abbreviations: HG, healthy group; OLP, olaparib-only group; ATOL, ATP + olaparib group; TPOL, TPP + olaparib group; MDA, malondialdehyde; tGSH, total glutathione; ATP, adenosine triphosphate; TPP, thiamine pyrophosphate.

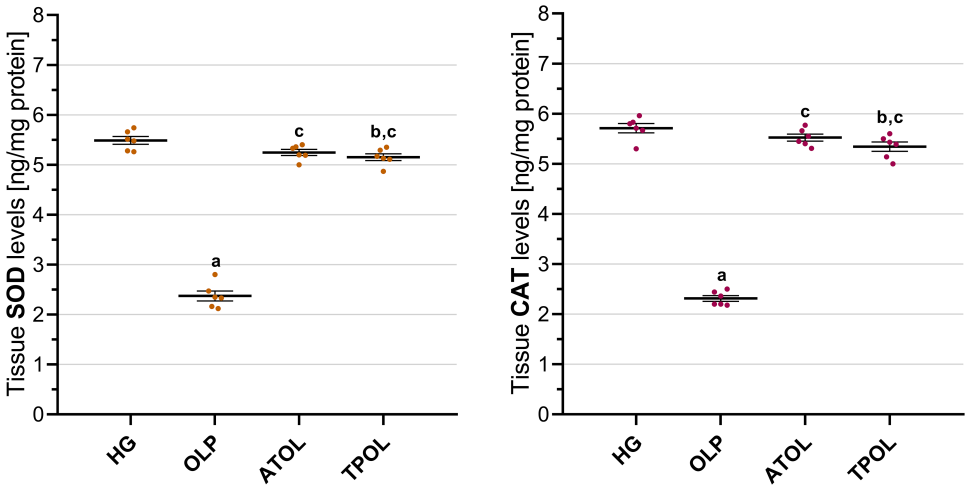


Figure 2 Effects of ATP, TPP, and olaparib on SOD and CAT levels in rat ovarian tissue.
Notes: Values represent mean ± SEM. Intergroup differences were assessed by one-way ANOVA followed by Tukey's honestly significant difference (HSD) post hoc test. [a] $p < 0.001$ vs HG; [b] $p < 0.05$ vs HG; [c] $p < 0.001$ vs OLP. n = 6 per group.
Abbreviations: HG, healthy group; OLP, olaparib-only group; ATOL, ATP + olaparib group; TPOL, TPP + olaparib group; SOD, superoxide dismutase; CAT, catalase; ATP, adenosine triphosphate; TPP, thiamine pyrophosphate.

Ovarian Tissue SOD and CAT Levels

As presented in Figure 2, olaparib treatment significantly reduced ovarian SOD levels in the OLP group (2.37 ± 0.10) compared with the HG group (5.49 ± 0.08) ($p < 0.001$). ATP and TPP administration prior to olaparib significantly attenuated the olaparib-induced reduction in SOD levels, yielding SOD levels of 5.25 ± 0.06 and 5.15 ± 0.07 in the ATOL and TPOL groups, respectively (both vs OLP, $p < 0.001$). No statistically significant difference was observed between the two treatment groups ($p = 0.835$). Although SOD levels in the ATOL group were comparable to that of healthy controls ($p = 0.165$), the TPOL group exhibited significantly lower SOD levels than the HG group ($p = 0.032$).

A comparable pattern was observed for CAT levels (Figure 2). Relative to healthy controls (5.71 ± 0.09), ovarian CAT levels were significantly decreased in the OLP group (2.31 ± 0.06) ($p < 0.001$). Pre-treatment with ATP (ATOL, 5.52 ± 0.07) or TPP (TPOL, 5.34 ± 0.09) significantly attenuated the olaparib-induced reduction in CAT levels (both vs OLP, $p < 0.001$). Consistent with the SOD findings, no significant difference was detected between the ATOL and TPOL groups ($p = 0.400$). Furthermore, CAT levels in the ATOL group remained comparable to that of the HG group ($p = 0.361$), whereas CAT levels in the TPOL group remained significantly lower than that observed in healthy controls ($p = 0.018$).

Ovarian Tissue IL-6 Levels

As illustrated in Figure 3, IL-6 levels were significantly higher in the OLP group (5.61 ± 0.07) than in the HG group (3.40 ± 0.07) ($p < 0.001$). Administration of ATP or TPP before olaparib significantly attenuated the olaparib-induced increase in IL-6 levels, yielding IL-6 levels of 3.62 ± 0.07 and 3.70 ± 0.07 in the ATOL and TPOL groups, respectively (both vs OLP, $p < 0.001$). No statistically significant difference was observed between the two treatment groups ($p = 0.867$). Although IL-6 levels in the ATOL group remained comparable to those of healthy animals ($p = 0.184$), the TPOL group exhibited significantly higher IL-6 levels than the HG group ($p = 0.042$).

Histopathological Findings

Histopathological findings paralleled the biochemical results (Table 1). Ovarian tissue from the HG exhibited normal architecture without evidence of follicular or parenchymal degeneration (Figure 4A), whereas the OLP group showed severe follicular and parenchymal degeneration (Figure 4B). Both ATP and TPP pretreatment significantly attenuated these olaparib-induced alterations, with ATP conferring significantly greater protection against follicular degeneration than TPP, whereas the two agents were comparably effective against parenchymal degeneration.

https://doi.org/10.2147/DDDT.S634516

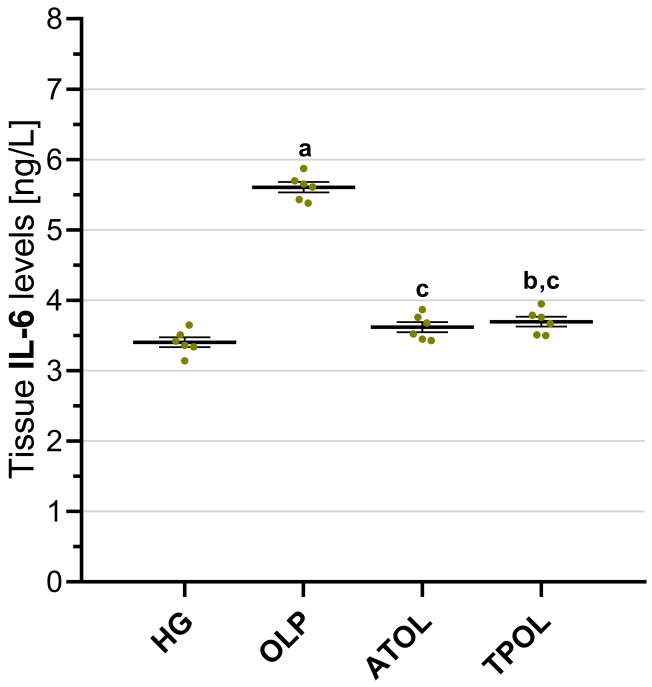


Figure 3 Effects of ATP, TPP, and olaparib on IL-6 levels in rat ovarian tissue.
Notes: Values represent mean ± SEM. Intergroup differences were assessed by one-way ANOVA followed by Tukey's honestly significant difference (HSD) post hoc test. [a] $p < 0.001$ vs HG; [b] $p < 0.05$ vs HG; [c] $p < 0.001$ vs OLP. n = 6 per group.
Abbreviations: HG, healthy group; OLP, olaparib-only group; ATOL, ATP + olaparib group; TPOL, TPP + olaparib group; IL-6, interleukin-6; ATP, adenosine triphosphate; TPP, thiamine pyrophosphate.

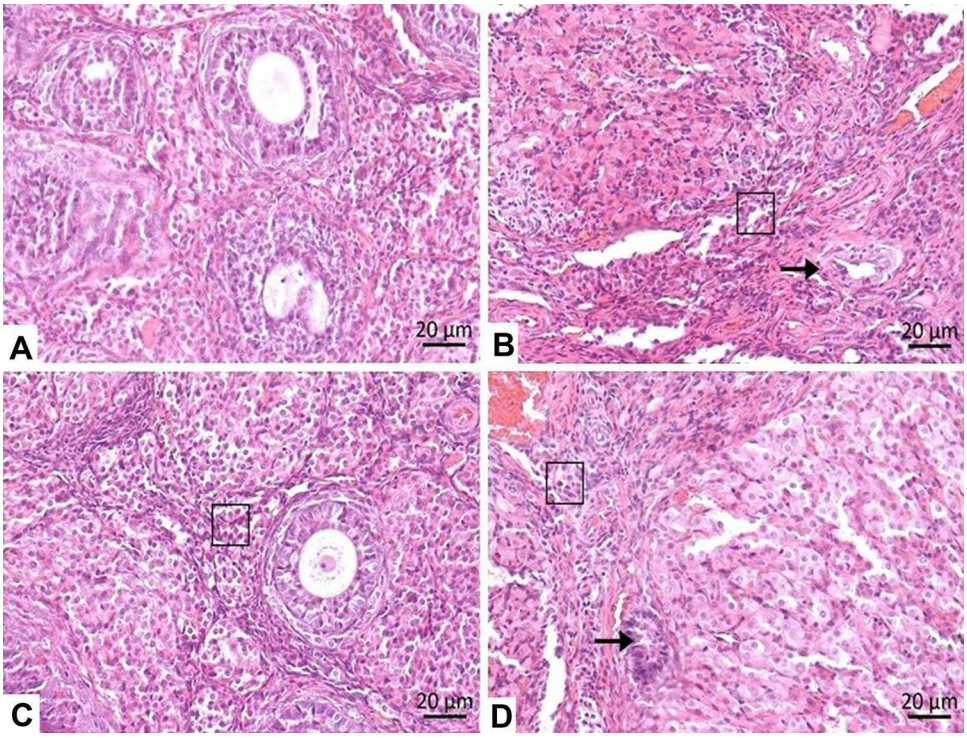


Figure 4 Representative photomicrographs of ovarian tissue sections stained with hematoxylin and eosin (H&E). (**A**) HG, normal histological appearance with preserved ovarian architecture. (**B**) OLP, severe follicular degeneration (grade 3, black arrow) with severe parenchymal degeneration (grade 3, open square). (**C**) ATOL, predominantly preserved follicular morphology with mild parenchymal degeneration (grade 1, open square). (**D**) TPOL, moderate follicular degeneration (grade 2, black arrow) accompanied by mild parenchymal degeneration (grade 1, open square).

 https://doi.org/10.2147/DDDT.S634516

Follicular degeneration was absent in the HG, with a median grade of 0 (range, 0–0), whereas severe follicular degeneration was observed in the OLP group, with a significantly higher median grade of 3 (range, 2–3) ($p < 0.05$). In the ATOL group, the median follicular degeneration grade was 0 (range, 0–1), indicating predominantly preserved follicular morphology, whereas the TPOL group exhibited moderate follicular degeneration, with a median grade of 2 (range, 1–2) (Figure 4C and 4D). Both treatment groups had significantly lower follicular degeneration grades than the OLP group ($p < 0.05$), and the grades also differed significantly between the ATOL and TPOL groups ($p < 0.05$). Moreover, follicular degeneration grades in the ATOL group were comparable to those in the HG group ($p > 0.05$) (Table 1).

Similarly, parenchymal degeneration was absent in the HG, with a median grade of 0 (range, 0–0), whereas severe parenchymal degeneration was observed in the OLP group, with a significantly higher median grade of 3 (range, 2–3) ($p < 0.05$). Pretreatment with both ATP and TPP markedly attenuated olaparib-induced parenchymal degeneration. Mild parenchymal degeneration was observed in both treatment groups, with a median grade of 1 (range, 0–2) in the ATOL group and 1 (range, 1–2) in the TPOL group (Figure 4C and 4D). Both treatment groups had significantly lower parenchymal degeneration grades than the OLP group ($p < 0.05$), although the grades remained significantly higher than those in the HG group ($p < 0.05$). No significant difference was observed between the ATOL and TPOL groups ($p > 0.05$) (Table 1).

Double Immunofluorescence Findings

Double immunofluorescence analysis demonstrated statistically significant intergroup differences in ovarian IRE1α, cleaved Caspase-3, LC3B, and NF-κB p65 immunopositivity grades (Table 2). Ovarian tissue from the HG exhibited absent IRE1α immunopositivity and mild cleaved Caspase-3 immunopositivity, whereas the OLP group showed markedly increased immunopositivity for both markers (Figure 5); a similar pattern of mild immunopositivity in the HG and marked olaparib-induced elevation was observed for LC3B and NF-κB p65 (Figure 6). For IRE1α and cleaved Caspase-3, both ATP and TPP pretreatment significantly attenuated these olaparib-associated increases, with comparable efficacy between the two agents. For LC3B and NF-κB p65, ATP pretreatment resulted in significantly lower immunopositivity grades than TPP pretreatment.

IRE1α immunopositivity was absent in the HG, with a median grade of 0 (range, 0–0), whereas severe IRE1α immunopositivity was observed in the OLP group, with a median grade of 3 (range, 2–3). In both the ATOL and TPOL groups, IRE1α immunopositivity was mild, with a median grade of 1 (range, 0–1) (Figure 5). Both ATP and TPP pretreatment significantly attenuated the olaparib-associated increase in IRE1α immunopositivity, with grades significantly lower than those in the OLP group ($p < 0.05$), although they remained significantly higher than those in the HG group ($p < 0.05$). No significant difference was observed between the ATOL and TPOL groups ($p > 0.05$) (Table 2).

Table 2 Double Immunofluorescence Signal Intensity Scores for Ovarian Injury Markers

Group	IRE1α	Cleaved Caspase-3	LC3B	NF-κB p65
HG	0 (0–0)	1 (1–1)	1 (0–1)	1 (0–1)
OLP	3 (2–3)[a]	3 (3–3)[a]	4 (3–4)[a]	4 (3–4)[a]
ATOL	1 (0–1)[a, b]	2 (1–2)[a, b]	2 (1–2)[a, b]	2 (1–2)[a, b]
TPOL	1 (0–1)[a, b]	2 (1–2)[a, b]	3 (2–3)[a, b, c]	3 (2–3)[a, b, c]

Notes: Data are expressed as median (min–max). Double immunofluorescence signal intensity and immunopositivity were evaluated semiquantitatively using a five-point scale (0 = absent, 1 = mild, 2 = moderate, 3 = severe, 4 = very severe). Pairwise comparisons were performed using the Mann–Whitney *U*-test (asymptotic, two-tailed) with Bonferroni correction applied for multiple comparisons. [a] $p < 0.05$ vs HG; [b] $p < 0.05$ vs OLP; [c] $p < 0.05$ vs ATOL. Each group comprised six animals (n = 6).

Abbreviations: HG, healthy group; OLP, olaparib-only group; ATOL, ATP + olaparib group; TPOL, TPP + olaparib group; ATP, adenosine triphosphate; TPP, thiamine pyrophosphate; IRE1α, inositol-requiring enzyme 1 alpha; cleaved Caspase-3, cleaved cysteine-aspartic protease 3; LC3B, light chain 3 beta; NF-κB p65, nuclear factor kappa B p65.

https://doi.org/10.2147/DDDT.S634516

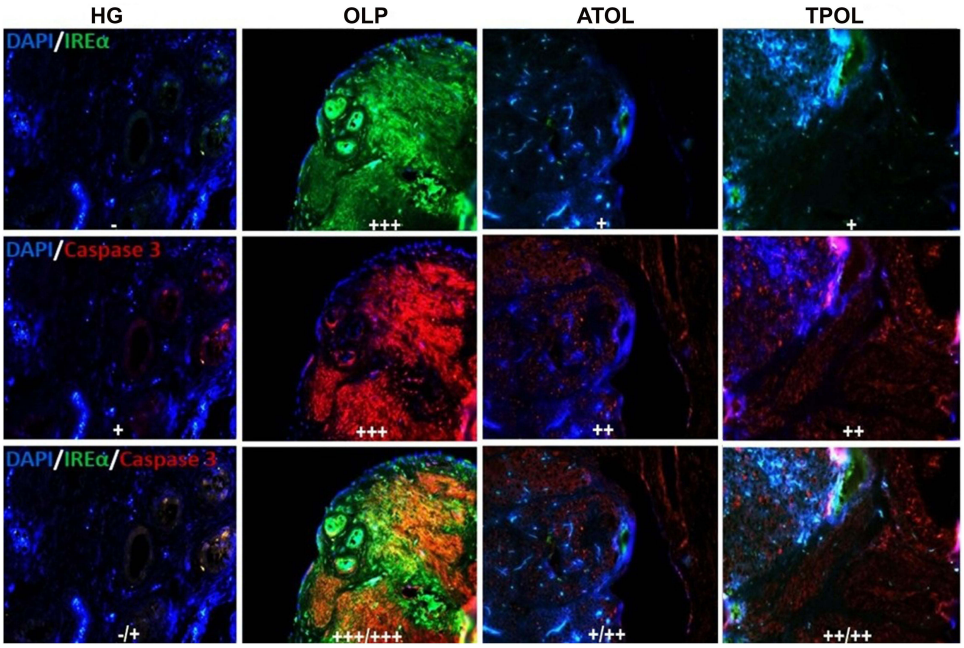


Figure 5 Representative immunofluorescence photomicrographs showing IRE1α (inositol-requiring enzyme 1 alpha, an endoplasmic reticulum stress sensor) and cleaved Caspase-3 (Asp175) (an effector caspase and marker of apoptotic activation) immunoreactivity in ovarian tissue sections across the HG, OLP, ATOL, and TPOL experimental groups. Immunoreactive staining intensity was assessed by semiquantitative scoring and classified into five grades: absent (−), mild (+), moderate (++), severe (+++), and very severe (++++). IRE1α immunoreactivity was visualized using fluorescein isothiocyanate (FITC), cleaved Caspase-3 immunoreactivity was detected using Alexa Fluor 594, and nuclei were counterstained with DAPI (4′,6-diamidino-2-phenylindole). In merged images, scores are presented as IRE1α/cleaved Caspase-3. ×40.
Abbreviations: HG, healthy group; OLP, olaparib-only group; ATOL, ATP + olaparib group; TPOL, TPP + olaparib group.

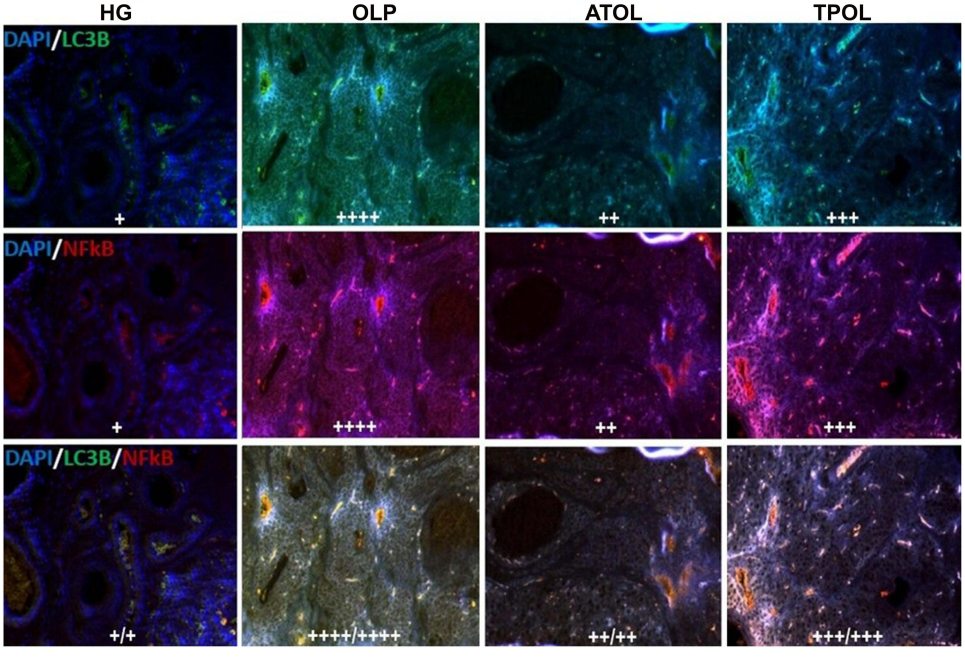


Figure 6 Representative immunofluorescence photomicrographs showing LC3B (microtubule-associated protein 1 light chain 3 beta, a marker of autophagosome formation) and NF-κB p65 (nuclear factor kappa-light-chain-enhancer of activated B cells, a key mediator of inflammatory signaling) immunoreactivity in ovarian tissue sections across the HG, OLP, ATOL, and TPOL experimental groups. Immunoreactive staining intensity was assessed by semiquantitative scoring and classified into five grades: absent (−), mild (+), moderate (++), severe (+++), and very severe (++++). LC3B immunoreactivity was visualized using fluorescein isothiocyanate (FITC), NF-κB p65 immunoreactivity was detected using Alexa Fluor 594, and nuclei were counterstained with DAPI (4′,6-diamidino-2-phenylindole). In merged images, scores are presented as LC3B/NF-κB p65. ×40.
Abbreviations: HG, healthy group; OLP, olaparib-only group; ATOL, ATP + olaparib group; TPOL, TPP + olaparib group.

Cleaved Caspase-3 immunopositivity was mild in the HG, with a median grade of 1 (range, 1–1), whereas severe immunopositivity was observed in the OLP group, with a median grade of 3 (range, 3–3). Both ATP and TPP pretreatment significantly attenuated the olaparib-associated increase in cleaved Caspase-3 immunopositivity, with moderate immunopositivity and a median grade of 2 (range, 1–2) in both the ATOL and TPOL groups (Figure 5). Both treatment groups had significantly lower cleaved Caspase-3 immunopositivity grades than the OLP group ($p < 0.05$), although the grades remained significantly higher than those in the HG group ($p < 0.05$). No significant difference was observed between the ATOL and TPOL groups ($p > 0.05$) (Table 2).

LC3B immunopositivity was mild in the HG, with a median grade of 1 (range, 0–1), whereas very severe LC3B immunopositivity was observed in the OLP group, with a median grade of 4 (range, 3–4). Both ATP and TPP pretreatment significantly attenuated the olaparib-associated increase in LC3B immunopositivity. The ATOL group exhibited moderate LC3B immunopositivity, with a median grade of 2 (range, 1–2), whereas the TPOL group exhibited severe immunopositivity, with a median grade of 3 (range, 2–3) (Figure 6). Both treatment groups had significantly lower LC3B immunopositivity grades than the OLP group ($p < 0.05$), although the grades remained significantly higher than those in the HG group ($p < 0.05$). Moreover, LC3B immunopositivity grades were significantly lower in the ATOL group than in the TPOL group ($p < 0.05$) (Table 2).

Similarly, NF-κB p65 immunopositivity was mild in the HG, with a median grade of 1 (range, 0–1), whereas very severe NF-κB p65 immunopositivity was observed in the OLP group, with a median grade of 4 (range, 3–4). Both ATP and TPP pretreatment significantly attenuated the olaparib-associated increase in NF-κB p65 immunopositivity. The ATOL group exhibited moderate NF-κB p65 immunopositivity, with a median grade of 2 (range, 1–2), whereas the TPOL group exhibited severe immunopositivity, with a median grade of 3 (range, 2–3) (Figure 6). Both treatment groups had significantly lower NF-κB p65 immunopositivity grades than the OLP group ($p < 0.05$), although the grades remained significantly higher than those in the HG group ($p < 0.05$). Moreover, NF-κB p65 immunopositivity grades were significantly lower in the ATOL group than in the TPOL group ($p < 0.05$) (Table 2).

Discussion

The present study investigated the potential protective effects of ATP and TPP against olaparib-induced ovarian injury in rats, employing biochemical, histopathological, and double immunofluorescence analyses to assess the underlying mechanisms of damage and protection. The findings of this study demonstrated that MDA levels, the end product of lipid peroxidation (LPO), were significantly increased in the olaparib-treated group. MDA is a reliable and well-established biomarker of oxidative stress.[53] Furthermore, PARP inhibitors are known to increase ROS production.[12] Our findings are consistent with previous reports demonstrating that olaparib promotes oxidative stress by enhancing ROS production.[28] In parallel with the increase in MDA levels observed following olaparib administration, tGSH levels were significantly decreased. Glutathione (GSH) is an endogenous antioxidant molecule that detoxifies hydrogen peroxide (H_2O_2), one of the major ROS, through direct reaction.[54] ATP is required for GSH synthesis, which plays a critical role in cellular defense against oxidative stress; in turn, GSH depletion leads to increased ROS levels, mitochondrial dysfunction, and ATP depletion.[55] The reduction in tGSH levels in the olaparib group indicates a diminished cellular defense against oxidative damage. These findings are consistent with previous reports demonstrating that olaparib reduces intracellular GSH levels.[12,56] Furthermore, SOD and CAT levels were significantly decreased in the olaparib group. As is well established, the superoxide anion ($\bullet O_2^-$), a type of ROS, is converted to H_2O_2 by SOD enzyme. H_2O_2 is subsequently reduced to non-toxic metabolites by the enzymes CAT and glutathione peroxidase.[57] SOD and CAT constitute the primary enzymatic defense system against oxidative stress, and their suppression results in cellular ROS accumulation and compromised cellular viability.[57–59] In our study, IL-6 levels were found to be significantly elevated in the olaparib-treated group. IL-6 is a pro-inflammatory cytokine that rises rapidly in response to infection or tissue injury.[60] Consistent with our findings, Guo et al reported that olaparib treatment was associated with elevated IL-6 levels.[61] It is now well established that oxidative stress and inflammation are mutually inducing processes; ROS activate NF-κB, thereby driving the production of pro-inflammatory mediators such as IL-6.[62] These findings suggest that olaparib administration may induce inflammation in ovarian tissue through this pathway.

The olaparib-induced increase in MDA levels was significantly suppressed in the ATP- and TPP-treated groups. Our findings from the ATP-treated group are consistent with previous studies demonstrating that decreased intracellular ATP levels are associated with increased MDA levels.[63] The significant suppression of MDA levels in the TPP-treated group is supported by evidence indicating that TPP functions as a cofactor in ATP synthesis.[37] In addition, Turan et al reported that TPP exerts antioxidant effects in liver tissue and prevents an increase in MDA levels.[64] Furthermore, olaparib-induced reduction in tGSH levels was prevented by ATP administration. This finding is consistent with the report by Kumbasar et al, which demonstrated that ATP administration significantly attenuated the olaparib-induced depletion of tGSH in ovarian tissue.[65] In addition, the decrease in tGSH levels associated with olaparib was also significantly attenuated by TPP administration. Similarly, literature reports demonstrating that TPP prevents the decline in GSH levels in an ethanol-induced oxidative stress model are supportive of the results observed in the present study.[38] As noted above, GSH synthesis is ATP-dependent.[55] ATP synthesis, in turn, occurs through reactions in which TPP participates as a cofactor.[45] An experimental study demonstrated that TPP increases ATP levels in ischemic cardiomyocytes.[66] Taken together, the ability of ATP to provide the energy required for GSH synthesis and the role of TPP as a cofactor in ATP production suggest that these two mechanisms may collectively contribute to the preservation of tGSH levels. Similarly, ATP and TPP administration significantly attenuated the reduction in SOD and CAT levels. Our findings from the ATP-treated group are consistent with previous studies demonstrating that activation of P2 receptors via extracellular ATP reduces oxidative damage in various cell types.[67] Thiamine is known to possess antioxidant properties.[35] Karatas et al reported that TPP alleviates erlotinib-associated oxidative and inflammatory responses and suppresses the decrease in SOD and CAT levels.[68] The preservation of SOD and CAT levels by ATP and TPP suggests that these agents may enhance cellular adaptive responses to oxidative stress. In our study, the olaparib-induced increase in IL-6 levels was also significantly suppressed by ATP and TPP administration. Previous studies have demonstrated the anti-inflammatory effects of ATP on blood cells.[33] In addition, studies have shown that TPP significantly reduces TNF-α and IL-6 levels in healthy rats.[69] It is also well established that thiamine deficiency is associated with the activation of inflammatory processes and increased ROS production.[35] Overall, these findings suggest that the reduction in IL-6 levels observed following ATP and TPP administration in our study is consistent with the existing literature. However, because ATP-only and TPP-only groups were not included, independent effects of ATP or TPP on these biochemical parameters cannot be excluded.

Histopathological examination revealed severe follicular and parenchymal degeneration in the olaparib group, consistent with the biochemical findings. These results are in line with previous reports indicating that PARP inhibitors induce cellular damage in ovarian tissue through the accumulation of DNA damage and apoptosis.[10,70] Consistent with the potential for olaparib-associated follicular injury, Kaseki et al recently demonstrated that olaparib administration significantly reduced primordial follicle numbers in Brca1-mutant rats, whereas this effect was not statistically significant in wild-type animals at the same dose. Their findings further indicated increased susceptibility of Brca1-mutant ovaries to oxidative stress and DNA damage-related responses, suggesting that genetic background may substantially influence the severity of olaparib-associated ovarian effects.[11] Nevertheless, the biochemical and molecular markers evaluated in the present study are not specific indicators of ovarian toxicity, and although the accompanying follicular and parenchymal degeneration provides morphological evidence of ovarian tissue injury, our findings do not directly establish impairment of ovarian reserve or reproductive function. Notably, follicular degeneration was markedly suppressed in the ATP-treated group. This finding is consistent with studies demonstrating the critical role of energy homeostasis in follicular survival.[71,72] Similarly, ATP administration has been shown to attenuate tramadol-induced stromal and follicular damage in ovarian tissue.[73] Although TPP administration also significantly reduced olaparib-induced ovarian damage, its effect appeared to be less pronounced than that of ATP. In a previous study, TPP was shown to significantly ameliorate morphological alterations in ovarian tissue subjected to ischemia–reperfusion injury.[74] As noted earlier, TPP is closely associated with cellular energy production due to its role as a cofactor for enzymes involved in mitochondrial energy metabolism.[37] The comparatively limited effect of TPP on histopathological improvement relative to ATP suggests that these two agents may not exert equivalent effects on energy metabolism in ovarian tissue. Nevertheless, in the absence of ATP-only and TPP-only groups, independent effects of these agents on ovarian morphology cannot be completely excluded.

In our study, a significant increase in IRE1α and caspase-3 immunopositivity was found in the olaparib group. As noted above, IRE1α is a transmembrane protein located in the ER that responds to ER stress by participating in the UPR. Under conditions of chronic ER stress, it can activate pathways that contribute to cellular degeneration and death.[75] Caspases are cysteine proteases that regulate cell death–related processes, including apoptosis, pyroptosis, and inflammation.[23] To date, no direct effect of olaparib on IRE1α has been reported in the literature. However, it is well established that cellular homeostasis is disrupted and ER stress responses are activated under conditions such as nutritional deficiency and sustained oxidative stress.[76] Olaparib-induced oxidative stress may contribute to the activation of endoplasmic reticulum stress pathways, thereby representing a plausible mechanism underlying the increased IRE1α immunopositivity observed in the present study. Consistent with our findings, Kim et al reported that PARP inhibitors can trigger pyroptosis through gasdermin-dependent pathways secondary to caspase-3 activation.[77] Similarly, Gao et al reported that olaparib exposure significantly increases caspase-3 activation in ovarian cancer cells.[19] Our results demonstrated increased LC3B and NF-κB immunopositivity in the olaparib group. LC3B is a protein that plays a central role in autophagy.[78] Autophagy, which is activated in response to conditions such as organelle damage, hypoxia, increased ROS levels, and ER stress, can contribute to cell death when these processes are excessively stimulated.[1,79,80] NF-κB is a family of transcription factors induced by stimuli such as infection, inflammatory cytokines, ischemia, and oxidative stress.[16] Previous studies reporting that olaparib suppresses DNA damage response mechanisms and induces autophagy support our findings.[1] On the other hand, interactions between caspases and NF-κB signaling pathways have been shown to play a critical role in cell survival.[81,82] Considering the evidence that olaparib enhances caspase-3 activation, it is conceivable that the NF-κB signaling pathway may be activated, at least in part, through this caspase-mediated mechanism.

In our study, ATP and TPP significantly suppressed the intensity of olaparib-induced IRE1α, caspase-3, LC3B, and NF-κB immunopositivity. In an experimental atherosclerosis model, preservation of intracellular ATP levels was shown to inhibit the ER stress–related IRE1α signaling pathway and to reduce caspase-3–mediated apoptosis and NF-κB immunopositivity in endothelial cells.[83] These reports demonstrating that the maintenance of energy homeostasis suppresses IRE1α and caspase-3 activation, as well as NF-κB-mediated inflammatory responses, are in agreement with and support our present findings. In addition, studies have reported that IRE1α plays a key role in ER stress–induced NF-κB activation.[84] AMPK has been reported to inhibit NF-κB and improve stress-induced inflammatory responses.[85] While decreased intracellular ATP levels lead to AMPK activation, increased ATP levels suppress AMPK activation.[85,86] Furthermore, a previous study has shown that intracellular ROS can indirectly activate AMPK through reductions in ATP concentrations.[85] It is plausible that ATP administration counteracted the increase in ROS levels induced by olaparib, thereby limiting oxidative stress and preventing the early activation of downstream cellular stress pathways. Similarly, a previous study has demonstrated that TPP significantly attenuates cyclophosphamide-induced NF-κB elevation in ovarian tissue.[87] The significant inhibition of olaparib-induced caspase-3 immunopositivity by ATP and TPP administration suggests attenuation of apoptotic activity. Caspase-3 is a key marker of apoptosis and represents the convergence point of intrinsic and extrinsic apoptotic pathways.[88] Gumusburun et al demonstrated in an experimental rat model that ATP attenuates tramadol-induced caspase-3 positivity in ovarian tissue.[73] Ciftel et al reported that elevated caspase-3 levels in the hepatic tissue of pyrazinamide-treated rats were significantly attenuated following co-administration of TPP.[89] Conversely, thiamine antagonists have been shown to increase DNA fragmentation and caspase-3 activation.[90] Moreover, AMPK has been shown to directly and indirectly induce autophagy.[85] The attenuation of olaparib-induced LC3B immunopositivity observed in the ATP-treated group may be attributed to the inhibitory effect of ATP on AMPK activity. Przygrodzka et al demonstrated that AMPK activates LC3B and induces autophagy in luteal cells.[91] Similarly, decreased intracellular ATP levels have been shown to activate AMPK, thereby initiating autophagy and increasing LC3B levels.[92] In the literature, there is no evidence demonstrating a direct association between TPP and LC3B. However, neurons exposed to thiamine deficiency exhibit autophagosome accumulation accompanied by increased LC3B levels, whereas these alterations have been shown to reverse following thiamine administration.[39] Moreover, TPP functions as an essential coenzyme and promotes ATP production by supporting the activity of the tricarboxylic acid (TCA) cycle.[93] In this context, the attenuation of olaparib-induced LC3B immunopositivity observed in our study may be attributed, at least in part, to the ATP-supporting effects of TPP. However, because ATP-only and TPP-only groups were

not included, independent effects of either compound on the immunofluorescence markers cannot be excluded; therefore, these mechanistic interpretations should be considered with appropriate caution. Our findings, together with evidence from the literature, suggest that energy homeostasis plays a critical role in maintaining cellular viability. Previous studies have reported that decreased ATP levels accelerate cell death and that disruption of energy homeostasis is closely associated with cellular damage.[94,95] Redegeld et al reported that a decrease in GSH alone does not lead to cell death, whereas the accompanying decline in ATP levels leads to loss of cell viability.[96]

Limitations and Future Perspectives

The present study has several methodological and conceptual limitations that should be acknowledged when interpreting the findings. First, a single fixed dose and a uniform treatment duration were employed for olaparib, ATP, and TPP; dose–response relationships and time-dependent effects, including those associated with prolonged or chronic olaparib exposure, were not systematically investigated. Second, ATP and TPP were administered as separate interventions and were not evaluated in combination; whether combinatorial administration would yield additive or synergistic protective effects remains to be determined. Third, ATP and TPP were administered intraperitoneally, whereas olaparib was administered by oral gavage; this difference in routes of administration may have resulted in divergent pharmacokinetic profiles with respect to absorption rate, volume of distribution, and tissue bioavailability, thereby complicating the interpretation of intergroup comparisons. Fourth, intracellular ATP and TPP levels in ovarian tissue were not directly measured, which limits the strength of the bioenergetic mechanistic conclusions and means that the proposed mechanism rests on indirect evidence. Fifth, mitochondrial bioenergetic parameters, including mitochondrial membrane potential, electron transport chain activity, and ATP synthase function, were not assessed, thereby restricting mechanistic elucidation of the relationship between oxidative stress and energy metabolism. Sixth, the stages of the estrous cycle were not monitored by vaginal cytology, which may have introduced biological variability and affected the interpretation of ovarian responses. Seventh, direct measures of ovarian reserve and reproductive function, including follicle quantification and staging, follicular development, follicular atresia, corpus luteum assessment, ovarian weight, ovulation, oocyte quality, pregnancy rates, and reproductive hormone levels such as FSH, LH, estradiol, and AMH, were not evaluated; consequently, whether the observed biochemical and histopathological protection translates into preserved ovarian reserve or reproductive function remains unclear. Eighth, as the study was conducted in a Wistar albino rat model, caution should be exercised when extrapolating the findings to human physiology, given that species-specific differences in ovarian hormonal responses, oxidative stress capacity, and drug metabolism may limit the direct clinical applicability of the present results. Ninth, the present experimental design did not include ATP-only or TPP-only groups in the absence of olaparib. Consequently, the study cannot determine whether ATP or TPP independently affects ovarian oxidative and inflammatory parameters, histopathological findings, or cellular stress-related markers under otherwise healthy conditions. Therefore, although differences between the OLP and ATOL or TPOL groups demonstrate treatment-associated effects during olaparib exposure, these differences cannot be attributed exclusively to attenuation of olaparib-induced injury, as independent effects of ATP or TPP on the measured outcomes cannot be excluded. Future studies incorporating ATP-only and TPP-only reference groups are required to distinguish these independent effects from effects specifically occurring in the context of olaparib exposure. Tenth, the once-daily dosing of ATP and TPP relative to the twice-daily olaparib regimen, together with the difference in administration routes noted above, represents an additional methodological consideration that may warrant attention in subsequent pharmacokinetic-oriented studies. Eleventh, the sample size (n = 6 per group) was determined without a formal a priori power analysis; therefore, the study may have had limited statistical power to detect more subtle intergroup differences. Twelfth, autophagic flux was not directly assessed. LC3B immunopositivity reflects LC3-II accumulation, which can result from either enhanced autophagosome formation or impaired autophagosome degradation; distinguishing between these possibilities would require dedicated flux assays. Thirteenth, ER-stress assessment was limited to IRE1α immunopositivity; a broader panel of established ER-stress/UPR markers was not evaluated. Accordingly, the present findings should be interpreted as evidence of IRE1α-associated ER stress signaling rather than comprehensive activation of the ER-stress/UPR pathway. Fourteenth, the total daily dose used in the present study (200 mg/kg/day) exceeds the doses evaluated in regulatory female reproductive toxicity studies in rats, and rat-specific plasma or ovarian olaparib concentrations for the regimen used here were not available in the

literature or measured in the present study. Therefore, direct pharmacokinetic equivalence between the present experimental regimen and clinically relevant human exposure cannot be established, and the ovarian injury observed in this study should be interpreted within the context of a high-dose experimental exposure paradigm rather than as a direct model of clinically relevant olaparib exposure. Addressing these limitations in future studies, through dose-optimization protocols, combination regimens, standardized pharmacokinetic profiling, direct bioenergetic measurements, autophagic flux assessment, broader ER-stress panel assessment, estrous cycle monitoring, the use of additional reference control arms, and functional reproductive outcome assessments, will strengthen the clinical relevance of the present findings and provide a basis for more comprehensive mechanistic interpretations.

Conclusion

The present study provides a direct comparative experimental evaluation of the protective effects of exogenous ATP and TPP against olaparib-induced ovarian injury in rats. Olaparib administration was associated with marked ovarian injury, characterized by significantly increased MDA and IL-6 levels and reduced tGSH, SOD, and CAT levels, a pattern consistent with enhanced oxidative stress, impaired antioxidant defense, and an increased inflammatory response. These biochemical alterations were accompanied by severe follicular and parenchymal degeneration, providing morphological evidence of ovarian tissue injury.

Double immunofluorescence analysis further demonstrated significantly increased IRE1α, cleaved Caspase-3, LC3B, and NF-κB p65 immunopositivity in olaparib-treated ovarian tissue, suggesting the involvement of IRE1α-related ER stress, cleaved Caspase-3-related apoptosis, LC3B-associated autophagy, and NF-κB-related inflammatory signaling in olaparib-associated ovarian injury. However, because these markers were assessed by semiquantitative immunopositivity alone, these findings should be interpreted as pathway-associated changes rather than evidence of causal pathway activation; notably, increased LC3B immunopositivity does not, by itself, establish increased autophagic flux.

Pretreatment with both ATP and TPP significantly attenuated the olaparib-induced biochemical and histopathological alterations and reduced IRE1α, cleaved Caspase-3, LC3B, and NF-κB p65 immunopositivity compared with olaparib treatment alone. These findings indicate that both ATP and TPP exert protective effects against olaparib-induced ovarian injury. ATP and TPP showed comparable effects across several measured outcomes; however, ATP showed greater protection than TPP for selected endpoints, specifically follicular degeneration and LC3B and NF-κB p65 immunopositivity.

The differences observed between ATP and TPP for selected endpoints may reflect differences in the mechanisms by which these compounds influence cellular energy metabolism. ATP may influence energy-dependent cellular processes more directly, whereas TPP primarily supports mitochondrial energy metabolism through its role as an enzymatic cofactor. However, this mechanistic interpretation remains hypothetical, as ovarian ATP and TPP levels and mitochondrial bioenergetic parameters were not directly assessed in the present study.

Because ovarian reserve and reproductive function were not directly assessed, the present findings should be interpreted as evidence of protection against biochemical, histopathological, and pathway-associated alterations in ovarian tissue rather than demonstrated preservation of fertility. Given the greater protection observed with ATP than with TPP for selected endpoints, further studies incorporating direct bioenergetic and functional pathway assessments, together with ovarian reserve and reproductive outcomes, are warranted to clarify the underlying mechanisms and determine the translational potential of ATP for protecting against olaparib-induced ovarian injury.

Use of Artificial Intelligence

The authors acknowledge the use of Claude (Anthropic, San Francisco, CA, USA; Version Claude Sonnet 4.6, accessed via Claude.ai Pro, 2026) and ChatGPT (OpenAI, San Francisco, CA, USA; Version GPT-5.3, accessed via ChatGPT Plus, 2026) for assistance with English language editing and manuscript clarity enhancement, given that English is not the native language of the authors, and for graphical abstract preparation. All AI-generated content was thoroughly reviewed, verified, and refined by the authors, who assume full responsibility for the accuracy and integrity of the final version.

Data Sharing Statement

Data are available from the corresponding author upon request. All data are included in this published article.

Author Contributions

All authors made a significant contribution to the work reported, whether that is in the conception, study design, execution, acquisition of data, analysis and interpretation, or in all these areas; took part in drafting, revising or critically reviewing the article; gave final approval of the version to be published; have agreed on the journal to which the article has been submitted; and agree to be accountable for all aspects of the work.

Funding

This research received no external funding.

Disclosure

The authors declare no conflicts of interest.

References

1. Arun B, Akar U, Gutierrez-Barrera AM, Hortobagyi GN, Ozpolat B. The PARP inhibitor AZD2281 (Olaparib) induces autophagy/mitophagy in BRCA1 and BRCA2 mutant breast cancer cells. *Int J Oncol*. 2015;47(1):262–268. doi:10.3892/ijo.2015.3003
2. Foo T, George A, Banerjee S. PARP inhibitors in ovarian cancer: an overview of the practice-changing trials. *Genes Chromosomes Cancer*. 2021;60(5):385–397. doi:10.1002/gcc.22935
3. Kovacs D, Vantus VB, Vamos E, et al. Olaparib: a Clinically Applied PARP Inhibitor Protects from Experimental Crohn's Disease and Maintains Barrier Integrity by Improving Bioenergetics through Rescuing Glycolysis in Colonic Epithelial Cells. *Oxid Med Cell Longev*. 2021;2021:7308897. doi:10.1155/2021/7308897
4. Elshazly AM, Nguyen TVV, Gewirtz DA. Is autophagy induction by PARP inhibitors a target for therapeutic benefit? *Oncol Res*. 2022;30(1):1–12. doi:10.32604/or.2022.026459
5. Ruiz-Schutz VC, Gomes LM, Mariano RC, et al. Risk of fatigue and anemia in patients with advanced cancer treated with olaparib: a meta-analysis of randomized controlled trials. *Crit Rev Oncol Hematol*. 2019;141:163–173. doi:10.1016/j.critrevonc.2019.06.012
6. Jin W, Yang Q, Zhang Z, Li J. Olaparib-associated toxicity in cancer patients: a systematic review and meta-analysis. *Eur J Clin Pharmacol*. 2025;81(1):65–81. doi:10.1007/s00228-024-03771-w
7. Tentori L, Lacal PM, Muzi A, et al. Poly(ADP-ribose) polymerase (PARP) inhibition or PARP-1 gene deletion reduces angiogenesis. *Eur J Cancer*. 2007;43(14):2124–2133. doi:10.1016/j.ejca.2007.07.010
8. Rajesh M, Mukhopadhyay P, Godlewski G, et al. Poly(ADP-ribose)polymerase inhibition decreases angiogenesis. *Biochem Biophys Res Commun*. 2006;350(4):1056–1062. doi:10.1016/j.bbrc.2006.09.160
9. Rajesh M, Mukhopadhyay P, Batkai S, et al. Pharmacological inhibition of poly(ADP-ribose) polymerase inhibits angiogenesis. *Biochem Biophys Res Commun*. 2006;350(2):352–357. doi:10.1016/j.bbrc.2006.09.049
10. Nakamura K, Takae S, Shiraishi E, Shinya K, Igualada AJ, Suzuki N. Poly (ADP-ribose) polymerase inhibitor exposure reduces ovarian reserve followed by dysfunction in granulosa cells. *Sci Rep*. 2020;10(1):17058. doi:10.1038/s41598-020-74087-9
11. Kaseki S, Sonehara R, Motooka Y, et al. Susceptibility of Brca1((L63X/+)) rat to ovarian reserve dissipation by chemotherapeutic agents to breast cancer. *Cancer Sci*. 2025;116(4):1139–1152. doi:10.1111/cas.16412
12. Hou D, Liu Z, Xu X, et al. Increased oxidative stress mediates the antitumor effect of PARP inhibition in ovarian cancer. *Redox Biol*. 2018;17:99–111. doi:10.1016/j.redox.2018.03.016
13. Liu Q, Gheorghiu L, Drumm M, et al. PARP-1 inhibition with or without ionizing radiation confers reactive oxygen species-mediated cytotoxicity preferentially to cancer cells with mutant TP53. *Oncogene*. 2018;37(21):2793–2805. doi:10.1038/s41388-018-0130-6
14. Shi C, Pan L, Amano S, Wu MY, Li C, Lin J. Co-Inhibition of PARP and STAT3 as a Promising Approach for Triple-Negative Breast Cancer. *Biomolecules*. 2025;15(7):1035. doi:10.3390/biom15071035
15. Chi L, Huan L, Zhang C, Wang H, Lu J. Adenosine receptor A2b confers ovarian cancer survival and PARP inhibitor resistance through IL-6-STAT3 signalling. *J Cell Mol Med*. 2023;27(15):2150–2164. doi:10.1111/jcmm.17802
16. Oeckinghaus A, Ghosh S. The NF-kappaB family of transcription factors and its regulation. *Cold Spring Harb Perspect Biol*. 2009;1(4):a000034. doi:10.1101/cshperspect.a000034
17. Hayden MS, Ghosh S. NF-kappaB in immunobiology. *Cell Res*. 2011;21(2):223–244. doi:10.1038/cr.2011.13
18. Jones SA, Jenkins BJ. Recent insights into targeting the IL-6 cytokine family in inflammatory diseases and cancer. *Nat Rev Immunol*. 2018;18(12):773–789. doi:10.1038/s41577-018-0066-7
19. Gao X, Yin Q, Wang Z. Olaparib Triggers Mitochondrial Fission Through the CDK5/Drp-1 Signaling Pathway in Ovarian Cancer Cells. *J Biochem Mol Toxicol*. 2025;39(6):e70273. doi:10.1002/jbt.70273
20. Junjappa RP, Patil P, Bhattarai KR, Kim HR, Chae HJ. IRE1alpha Implications in Endoplasmic Reticulum Stress-Mediated Development and Pathogenesis of Autoimmune Diseases. *Front Immunol*. 2018;9:1289. doi:10.3389/fimmu.2018.01289
21. Schonthal AH. Endoplasmic reticulum stress: its role in disease and novel prospects for therapy. *Scientifica*. 2012;2012:857516. doi:10.6064/2012/857516
22. Elmore S. Apoptosis: a review of programmed cell death. *Toxicol Pathol*. 2007;35(4):495–516. doi:10.1080/01926230701320337

23. Julien O, Wells JA. Caspases and their substrates. *Cell Death Differ*. 2017;24(8):1380–1389. doi:10.1038/cdd.2017.44
24. Parrish AB, Freel CD, Kornbluth S. Cellular mechanisms controlling caspase activation and function. *Cold Spring Harb Perspect Biol*. 2013;5 (6):8672. doi:10.1101/cshperspect.a008672
25. Shi Y, Zhou F, Jiang F, Lu H, Wang J, Cheng C. PARP inhibitor reduces proliferation and increases apoptosis in breast cancer cells. *Chin J Cancer Res*. 2014;26(2):142–147. doi:10.3978/j.issn.1000-9604.2014.02.13
26. Weston VJ, Oldreive CE, Skowronska A, et al. The PARP inhibitor olaparib induces significant killing of ATM-deficient lymphoid tumor cells in vitro and in vivo. *Blood*. 2010;116(22):4578–4587. doi:10.1182/blood-2010-01-265769
27. Samarasekera G, Go NE, Choutka C, et al. Caspase 3 and caspase 7 promote cytoprotective autophagy and the DNA damage response during non-lethal stress conditions in human breast cancer cells. *PLoS Biol*. 2025;23(2):e3003034. doi:10.1371/journal.pbio.3003034
28. Santiago-O'Farrill JM, Weroha SJ, Hou X, et al. Poly(adenosine diphosphate ribose) polymerase inhibitors induce autophagy-mediated drug resistance in ovarian cancer cells, xenografts, and patient-derived xenograft models. *Cancer*. 2020;126(4):894–907. doi:10.1002/cncr.32600
29. Bulut S, Süleyman H. Relationship between Oxidative Stress and Cellular Adenosine Triphosphate Levels. *Recent Trends Pharmacol*. 2024;2 (2):79–82. doi:10.62425/rtpharma.1467636
30. Nankivell MC, Rosenfeldt F, Pipingas A, Pase MP, Reddan JM, Stough C. Coenzyme Q10 and Cognition: a Review. *Nutrients*. 2025;17(17):2896. doi:10.3390/nu17172896
31. Liang H, Van Remmen H, Frohlich V, Lechleiter J, Richardson A, Ran Q. Gpx4 protects mitochondrial ATP generation against oxidative damage. *Biochem Biophys Res Commun*. 2007;356(4):893–898. doi:10.1016/j.bbrc.2007.03.045
32. Dunn J, Grider MH. Physiology, Adenosine Triphosphate. In: *StatPearls [Internet]*. Treasure Island (FL): StatPearls Publishing; 2026. PMID: 31985968.
33. Swennen EL, Dagnelie PC, Bast A. ATP inhibits hydroxyl radical formation and the inflammatory response of stimulated whole blood even under circumstances of severe oxidative stress. *Free Radic Res*. 2006;40(1):53–58. doi:10.1080/10715760500364298
34. Kwon J, Kim J, Kim KI. Crosstalk between endoplasmic reticulum stress response and autophagy in human diseases. *Anim Cells Syst*. 2023;27 (1):29–37. doi:10.1080/19768354.2023.2181217
35. Kazmierczak-Baranska J, Halczuk K, Karwowski BT. Thiamine (Vitamin B1)-An Essential Health Regulator. *Nutrients*. 2025;17(13):2206. doi:10.3390/nu17132206
36. Huang W, Qin J, Liu D, et al. Reduced thiamine binding is a novel mechanism for TPK deficiency disorder. *Mol Genet Genomics*. 2019;294 (2):409–416. doi:10.1007/s00438-018-1517-3
37. Subramanian VS, Nabokina SM, Lin-Moshier Y, Marchant JS, Said HM. Mitochondrial uptake of thiamin pyrophosphate: physiological and cell biological aspects. *PLoS One*. 2013;8(8):e73503. doi:10.1371/journal.pone.0073503
38. Ucak T, Karakurt Y, Tasli G, et al. The effects of thiamine pyrophosphate on ethanol induced optic nerve damage. *BMC Pharmacol Toxicol*. 2019;20(1):40. doi:10.1186/s40360-019-0319-5
39. Meng Y, Yong Y, Yang G, et al. Autophagy alleviates neurodegeneration caused by mild impairment of oxidative metabolism. *J Neurochem*. 2013;126(6):805–818. doi:10.1111/jnc.12268
40. Ma Y, Elmhadi M, Wang C, Zhang H, Wang HR. Dietary supplementation of thiamine down-regulates the expression of mitophagy and endoplasmic reticulum stress-related genes in the rumen epithelium of goats during high-concentrate diet feeding. *Ital J Anim Sci*. 2021;20 (1):2220–2231. doi:10.1080/1828051x.2021.1985944
41. Baykan AR, Cerrah S, Kartal Baykan E, et al. Potential Hepatoprotective Effects of Adenosine Triphosphate Against Olaparib-Induced Oxidative Liver Injury: an Experimental Rat Model. *Drug Des Devel Ther*. 2026;20:613667. doi:10.2147/DDDT.S613667
42. European Parliament, Council of the European Union. Directive 2010/63/EU of the European Parliament and of the Council of 22 September 2010 on the protection of animals used for scientific purposes. *Off J Eur Union*. 2010;L276:33–79.
43. du Sert N P, Hurst V, Ahluwalia A, et al. The ARRIVE guidelines 2.0: updated guidelines for reporting animal research. *PLoS Biol*. 2020;18(7): e3000410. doi:10.1371/journal.pbio.3000410
44. Kiani AK, Pheby D, Henehan G, et al. Ethical considerations regarding animal experimentation. *J Prev Med Hyg*. 2022;63(2 Suppl 3):E255–E266. doi:10.15167/2421-4248/jpmh2022.63.2S3.2768
45. Ozgodek HB, Ince R, Kahramanlar AA, et al. A Comparative Evaluation of the Therapeutic Effects of Adenosine Triphosphate, Coenzyme Q10, Pyridoxine, and Thiamine Pyrophosphate in a Linezolid-Induced Peripheral Neuropathic Pain Model in Rats. *Pharmaceuticals*. 2026;19(2):341. doi:10.3390/ph19020341
46. Onk D, Mammadov R, Suleyman B, et al. The effect of thiamine and its metabolites on peripheral neuropathic pain induced by cisplatin in rats. *Exp Anim*. 2018;67(2):259–269. doi:10.1538/expanim.17-0090
47. Fakirullahoglu M, Temiz A, Yeni M, et al. ATP attenuates olaparib-induced gastric damage in rats. *Front Pharmacol*. 2026;17:1847232. doi:10.3389/fphar.2026.1847232
48. To C, Kim EH, Royce DB, et al. The PARP inhibitors, veliparib and olaparib, are effective chemopreventive agents for delaying mammary tumor development in BRCA1-deficient mice. *Cancer Prev Res*. 2014;7(7):698–707. doi:10.1158/1940-6207.CAPR-14-0047
49. Sun K, Mikule K, Wang Z, et al. A comparative pharmacokinetic study of PARP inhibitors demonstrates favorable properties for niraparib efficacy in preclinical tumor models. *Oncotarget*. 2018;9(98):37080–37096. doi:10.18632/oncotarget.26354
50. Zhou D, Li J, Bui K, et al. Bridging Olaparib Capsule and Tablet Formulations Using Population Pharmacokinetic Meta-analysis in Oncology Patients. *Clin Pharmacokinet*. 2019;58(5):615–625. doi:10.1007/s40262-018-0714-x
51. American Veterinary Medical Association. AVMA Guidelines for the Euthanasia of Animals: 2020 Edition. Schaumburg, IL: AVMA; 2020. Available from: https://www.avma.org/sites/default/files/2020-02/Guidelines-on-Euthanasia-2020.pdf. Accessed Sep 07, 2026.
52. Bradford MM. A rapid and sensitive method for the quantitation of microgram quantities of protein utilizing the principle of protein-dye binding. *Anal Biochem*. 1976;72:248–254. doi:10.1016/0003-2697(76)90527-3
53. Qasim MN, Mahmood HG. Assessment of Malondialdehyde as a Biomarker of Oxidative Stress and Its Correlation with 25-hydroxy Vitamin D_3 in Women with Polycystic Ovary Syndromeoxy Vitamin D_3. *J Faculty Med Baghdad*. 2025;67(3):330–337. doi:10.32007/jfacmedbaghdad3141
54. Murray RK, Granner DK, Mayes PA, Rodwell VW. Harper's illustrated biochemistry. In: *Lange Medical Books/Mcgraw-Hill*. 26th edn; 2003:693.
55. Lu SC. Regulation of glutathione synthesis. *Mol Aspects Med*. 2009;30(1–2):42–59. doi:10.1016/j.mam.2008.05.005

56. Hong T, Lei G, Chen X, et al. PARP inhibition promotes ferroptosis via repressing SLC7A11 and synergizes with ferroptosis inducers in BRCA-proficient ovarian cancer. *Redox Biol*. 2021;42:101928. doi:10.1016/j.redox.2021.101928
57. Jomova K, Alomar SY, Alwasel SH, Nepovimova E, Kuca K, Valko M. Several lines of antioxidant defense against oxidative stress: antioxidant enzymes, nanomaterials with multiple enzyme-mimicking activities, and low-molecular-weight antioxidants. *Arch Toxicol*. 2024;98(5):1323–1367. doi:10.1007/s00204-024-03696-4
58. Lee J, Kim J, Lee R, et al. Therapeutic strategies for liver diseases based on redox control systems. *Biomed Pharmacother*. 2022;156:113764. doi:10.1016/j.biopha.2022.113764
59. Cui Z, He F, Li X, et al. Response pathways of superoxide dismutase and catalase under the regulation of triclocarban-triggered oxidative stress in Eisenia foetida: comprehensive mechanism analysis based on cytotoxicity and binding model. *Sci Total Environ*. 2023;854:158821. doi:10.1016/j.scitotenv.2022.158821
60. Tanaka T, Narazaki M, Masuda K, Kishimoto T. Regulation of IL-6 in Immunity and Diseases. *Adv Exp Med Biol*. 2016;941:79–88. doi:10.1007/978-94-024-0921-5_4
61. Guo H, Lu R, Yuan S, et al. Activation of cGAS confers PARP inhibitor resistance in ovarian cancer via the TBK1-IRF3 axis. *Int J Clin Exp Pathol*. 2024;17(11):429–438. doi:10.62347/XOPN6908
62. Manful CF, Fordjour E, Ikumoinein E, Abbey L, Thomas R. Therapeutic Strategies Targeting Oxidative Stress and Inflammation: a Narrative Review. *Biochem*. 2025;5(4):35. doi:10.3390/biochem5040035
63. Schutt F, Aretz S, Auffarth GU, Kopitz J. Moderately reduced ATP levels promote oxidative stress and debilitate autophagic and phagocytic capacities in human RPE cells. *Invest Ophthalmol Vis Sci*. 2012;53(9):5354–5361. doi:10.1167/iovs.12-9845
64. Turan MI, Siltelioglu Turan I, Mammadov R, Altinkaynak K, Kisaoglu A. The effect of thiamine and thiamine pyrophosphate on oxidative liver damage induced in rats with cisplatin. *Biomed Res Int*. 2013;2013:783809. doi:10.1155/2013/783809
65. Kumbasar S, Cetin N, Yapca OE, et al. Exogenous ATP administration prevents ischemia/reperfusion-induced oxidative stress and tissue injury by modulation of hypoxanthine metabolic pathway in rat ovary. *Ciencia Rural*. 2014;44(7):1257–1263. doi:10.1590/0103-8478cr20131006
66. Yamada Y, Kusakari Y, Akaoka M, et al. Thiamine treatment preserves cardiac function against ischemia injury via maintaining mitochondrial size and ATP levels. *J Appl Physiol*. 2021;130(1):26–35. doi:10.1152/japplphysiol.00578.2020
67. Satoh E, Tsukimoto M, Kojima S. Involvement of P2Y receptors in the protective effect of ATP towards the cell damage in HaCaT cells exposed to H(2)O(2). *J Toxicol Sci*. 2011;36(6):741–750. doi:10.2131/jts.36.741
68. Karatas E, Yavuzer B, Demir O, et al. Protective Role of Thiamine Pyrophosphate Against Erlotinib-Induced Oxidative and Inflammatory Damage in Rat Optic Nerve. *Biomedicines*. 2025;13(11):2614. doi:10.3390/biomedicines13112614
69. Mahdavifard S, Nakhjavani M. Thiamine pyrophosphate improved vascular complications of diabetes in rats with type 2 diabetes by reducing glycation, oxidative stress, and inflammation markers. *Med J Islam Repub Iran*. 2020;34:47. doi:10.34171/mjiri.34.47
70. Li J, Li Q, Zhang L, Zhang S, Dai Y. Poly-ADP-ribose polymerase (PARP) inhibitors and ovarian function. *Biomed Pharmacother*. 2023;157:114028. doi:10.1016/j.biopha.2022.114028
71. Marynowicz W, Glod P, Maduzia D, Gogola-Mruk J, Ptak A. Energy imbalance in oPOI ovarian granulosa cells is linked to reduced glucose bioavailability and metabolism. *Reprod Biol Endocrinol*. 2025;23(1):96. doi:10.1186/s12958-025-01426-8
72. Khodamoradi K, Khosravizadeh Z, Rashidi Z, Talebi A, Hassanzadeh G. The role of mitochondria in premature ovarian failure: a review. *J Contemp Med Sci*. 2020;6(1):1–7. doi:10.22317/jcms.02202001
73. Gumusburun N, Delibasi IB, Bulut S, et al. Association of Tramadol-Induced Ovarian Damage and Reproductive Dysfunction with Adenosine Triphosphate and the Protective Role of Exogenous ATP Treatment. *Pharmaceuticals*. 2025;18(2):216. doi:10.3390/ph18020216
74. Demiryilmaz I, Sener E, Cetin N, Altuner D, Akcay F, Suleyman H. A comparative investigation of biochemical and histopathological effects of thiamine and thiamine pyrophosphate on ischemia-reperfusion induced oxidative damage in rat ovarian tissue. *Arch Pharm Res*. 2013;36(9):1133–1139. doi:10.1007/s12272-013-0173-8
75. Hetz C, Papa FR. The Unfolded Protein Response and Cell Fate Control. *Mol Cell*. 2018;69(2):169–181. doi:10.1016/j.molcel.2017.06.017
76. Qi Z, Chen L. Endoplasmic Reticulum Stress and Autophagy. *Adv Exp Med Biol*. 2019;1206:167–177. doi:10.1007/978-981-15-0602-4_8
77. Kim C, Wang XD, Jang S, Yu Y. PARP1 inhibitors induce pyroptosis via caspase 3-mediated gasdermin E cleavage. *Biochem Biophys Res Commun*. 2023;646:78–85. doi:10.1016/j.bbrc.2023.01.055
78. Hwang HJ, Ha H, Lee BS, Kim BH, Song HK, Kim YK. LC3B is an RNA-binding protein to trigger rapid mRNA degradation during autophagy. *Nat Commun*. 2022;13(1):1436. doi:10.1038/s41467-022-29139-1
79. Cubillos-Ruiz JR, Bettigole SE, Glimcher LH. Tumorigenic and Immunosuppressive Effects of Endoplasmic Reticulum Stress in Cancer. *Cell*. 2017;168(4):692–706. doi:10.1016/j.cell.2016.12.004
80. Chen Q, Kang J, Fu C. The Independence of and associations among apoptosis, autophagy, and necrosis. *Signal Transduct Target Ther*. 2018;3:18. doi:10.1038/s41392-018-0018-5
81. Lamkanfi M, Festjens N, Declercq W, Vanden Berghe T, Vandenabeele P. Caspases in cell survival, proliferation and differentiation. *Cell Death Differ*. 2007;14(1):44–55. doi:10.1038/sj.cdd.4402047
82. Flusberg DA, Sorger PK. Surviving apoptosis: life-death signaling in single cells. *Trends Cell Biol*. 2015;25(8):446–458. doi:10.1016/j.tcb.2015.03.003
83. Zou F, Baba O, Horie T, et al. KUS121, a novel VCP modulator, attenuates atherosclerosis development by reducing ER stress and inhibiting glycolysis through the maintenance of ATP levels in endothelial cells. *Atherosclerosis*. 2025;405:119223. doi:10.1016/j.atherosclerosis.2025.119223
84. Hu P, Han Z, Couvillon AD, Kaufman RJ, Exton JH. Autocrine tumor necrosis factor alpha links endoplasmic reticulum stress to the membrane death receptor pathway through IRE1alpha-mediated NF-kappaB activation and down-regulation of TRAF2 expression. *Mol Cell Biol*. 2006;26(8):3071–3084. doi:10.1128/MCB.26.8.3071-3084.2006
85. Sharma A, Anand SK, Singh N, Dwivedi UN, Kakkar P. AMP-activated protein kinase: an energy sensor and survival mechanism in the reinstatement of metabolic homeostasis. *Exp Cell Res*. 2023;428(1):113614. doi:10.1016/j.yexcr.2023.113614
86. Xiao B, Heath R, Saiu P, et al. Structural basis for AMP binding to mammalian AMP-activated protein kinase. *Nature*. 2007;449(7161):496–500. doi:10.1038/nature06161

87. Ozer M, Ince S, Gundogdu B, et al. Effect of thiamine pyrophosphate on cyclophosphamide-induced oxidative ovarian damage and reproductive dysfunction in female rats. *Adv Clin Exp Med*. 2022;31(2):129–137. doi:10.17219/acem/142535
88. Lossi L, Castagna C, Merighi A. Caspase-3 Mediated Cell Death in the Normal Development of the Mammalian Cerebellum. *Int J Mol Sci*. 2018;19(12):3999. doi:10.3390/ijms19123999
89. Ciftel S, Ciftel S, Altuner D, et al. Effects of adenosine triphosphate, thiamine pyrophosphate, melatonin, and liv-52 on subacute pyrazinamide proliferation hepatotoxicity in rats. *BMC Pharmacol Toxicol*. 2025;26(1):67. doi:10.1186/s40360-025-00901-7
90. Chornyy S, Parkhomenko J, Chorna N. Thiamine deficiency caused by thiamine antagonists triggers upregulation of apoptosis inducing factor gene expression and leads to caspase 3-mediated apoptosis in neuronally differentiated rat PC-12 cells. *Acta Biochim Pol*. 2007;54(2):315–322.
91. Przygrodzka E, Monaco CF, Plewes MR, et al. Protein Kinase A and 5' AMP-Activated Protein Kinase Signaling Pathways Exert Opposite Effects on Induction of Autophagy in Luteal Cells. *Front Cell Dev Biol*. 2021;9:723563. doi:10.3389/fcell.2021.723563
92. Che L, Yang X, Ge C, et al. Loss of BRUCE reduces cellular energy level and induces autophagy by driving activation of the AMPK-ULK1 autophagic initiating axis. *PLoS One*. 2019;14(5):e0216553. doi:10.1371/journal.pone.0216553
93. Yamada Y, Ishimaru T, Harashima H. Validation of a therapeutic strategy involving the mitochondrial delivery of thiamine pyrophosphate using brain damage induced mouse model. *Clin Transl Discovery*. 2022;2(2):e43. doi:10.1002/ctd2.43
94. Del Nagro C, Xiao Y, Rangell L, Reichelt M, O'Brien T. Depletion of the central metabolite NAD leads to oncosis-mediated cell death. *J Biol Chem*. 2014;289(51):35182–35192. doi:10.1074/jbc.M114.580159
95. Singer M. Critical illness and flat batteries. *Crit Care*. 2017;21(Suppl 3):309. doi:10.1186/s13054-017-1913-9
96. Redegeld FA, Moison RM, Koster AS, Noordhoek J. Depletion of ATP but not of GSH affects viability of rat hepatocytes. *Eur J Pharmacol*. 1992;228(4):229–236. doi:10.1016/0926-6917(92)90034-a

Drug Design, Development and Therapy

Dovepress
Taylor & Francis Group

Publish your work in this journal

Drug Design, Development and Therapy is an international, peer-reviewed open-access journal that spans the spectrum of drug design and development through to clinical applications. Clinical outcomes, patient safety, and programs for the development and effective, safe, and sustained use of medicines are a feature of the journal, which has also been accepted for indexing on PubMed Central. The manuscript management system is completely online and includes a very quick and fair peer-review system, which is all easy to use. Visit http://www.dovepress.com/testimonials.php to read real quotes from published authors.

Submit your manuscript here: https://www.dovepress.com/drug-design-development-and-therapy-journal